

## A UHF Wind Profiler for the Boundary Layer: Brief Description and Initial Results

W. L. ECKLUND, D. A. CARTER AND B. B. BALSLEY

*Aeronomy Laboratory, National Oceanic and Atmospheric Administration, Boulder, Colorado*

(Manuscript received 16 September 1987, in final form 20 November 1987)

### ABSTRACT

In this paper we describe a boundary layer radar recently developed at NOAA's Aeronomy Laboratory. This radar extends wind profiler technology by using a small, relatively inexpensive radar to provide continuous, high-resolution wind measurements in the first few kilometers of the atmosphere. Although the radar was developed for use in a "hybrid" mode with existing 50 MHz profilers in the tropical Pacific, the system can equally well be a stand-alone device to study boundary layer problems.

### 1. Introduction

Wind profiling by the use of sensitive pulsed Doppler radars is now well established (Balsley and Gage 1982; Strauch et al. 1984). Wind profilers typically operate in the frequency range from 40 to 915 MHz, while specific studies have utilized radar frequencies as high as 3000 MHz.

For both historic and economic reasons, a number of wind profilers have been built to operate from 40 to 55 MHz. Radars operating in this lower part of the VHF (30 to 300 MHz) band have some distinct advantages over radars operating at higher frequencies. One important advantage is that atmospheric scattering at lower VHF is nearly always stronger than scattering from hydrometeors. Consequently, vertical atmospheric motions can be measured at these frequencies, even during rainfall (Fukao et al. 1985). These radars also are able to detect stable layers with the practical result that they can monitor the height of the tropopause on a continuous basis (Gage et al. 1986).

However, lower VHF wind profilers have a serious limitation, namely their inability to measure high-resolution winds in the first kilometer or so of the lower atmosphere. This minimum height limitation arises from various factors, including 1) receiver overload due to strong ground clutter and internal reflections in large antenna arrays, 2) the inherent inability of large aperture arrays operating in this frequency range to form well-defined beams in the first kilometer or so above the array, and 3) the practical system bandwidth limitation; e.g., a 75 meter resolution requires a transmitted pulse width of 0.5  $\mu$ s and a corresponding bandwidth of about 2 MHz.

A number of meteorological studies would be greatly facilitated by continuous high-resolution wind profiles in the first 1–2 km of the atmosphere. One obvious example is the study of boundary layer convergence processes and their relationship to atmospheric convection. Other equally important subjects include surface frontal passages, mountain drainage flows, urban pollution studies, and airport-related studies of wind shear and downburst dynamics. Clearly, the extension of current profiler technology to the lowest portion of the atmosphere is important.

In this paper we describe a boundary layer radar (BLR) system recently developed by NOAA's Aeronomy Laboratory to provide continuous, high-resolution wind measurements in the first few kilometers of the atmosphere. Our initial need is to operate, in conjunction with existing 50 MHz profilers in the tropical Pacific, in a "hybrid" mode to provide wind profiles in the boundary layer and in the troposphere and lower stratosphere. The BLR system, however, can equally well be a stand-alone device to study many of the boundary layer problems mentioned above.

In the following sections we outline the general features of the BLR system and show sample wind profiles obtained under a variety of conditions, both in Colorado and at our tropical wind profiler site at Christmas Island (Republic of Kiribati) in the central equatorial Pacific.

### 2. Design considerations

The BLR described in this report was designed to meet the following requirements:

1. The system should use a simple, inexpensive, small antenna with a far field of preferably less than 100 m.
2. The antenna should be low to the ground or shielded to minimize ground clutter.

*Corresponding author address:* Mr. Warner L. Ecklund, NOAA/ERL, 325 Broadway, Boulder, CO 80303.

3. System recovery should be fast enough to obtain useful measurements at heights at least as low as 100 m above ground.

4. The system should have a height resolution of 100 m or better.

5. The BLR should be sensitive enough to obtain data to a height of 2–3 km under typical atmospheric conditions.

Most of the general profiler design concepts have been covered in Balsley and Gage (1982). These authors show that the high spatial resolution and fast system recovery outlined above require operation at frequencies near 1000 MHz. In addition, the antenna requirements listed above also could best be met by operating in the middle of the UHF (300 to 3000 MHz) band. Consequently, a frequency of 915 MHz was selected since NOAA's Wave Propagation Laboratory has successfully operated a large wind profiler at this frequency near Denver's Stapleton Airport since 1983 (Strauch et al. 1985).

The main disadvantage of operating a wind profiler at the relatively high frequency of 915 MHz is the enhanced sensitivity to hydrometeors. Under precipitation conditions (or in heavy clouds), the radar signal will be dominated by scattering from hydrometeors, and, consequently, the determination of vertical air motion will not be possible (since the radar measures the hydrometeor fall speed instead). The radar-measured fall speed may differ from the terminal velocity of the hydrometeors due to vertical wind. To the extent that hydrometeors are advected horizontally by the mean winds as they fall, however, it is still possible to obtain a profile of the horizontal wind (Wuertz et al. 1988). In general, wind profilers require that the wind field be relatively uniform over the area scanned by the radar antenna beams. Profiling winds under precipitation conditions requires not only that the wind field be uniform, but also that the precipitation field be relatively uniform over the scanned area. This suggests that a 915 MHz radar will probably be able to obtain reasonably good wind profiles under stratiform precipitation conditions, but the wind profiles will be compromised to some degree when winds and precipitation are structured (as in rapidly moving thunderstorms). This contention is supported by examples of wind profiles obtained under various conditions presented later in this report.

### 3. System description

#### a. Block diagram

A block diagram of the boundary layer radar is shown in Fig. 1. The units to the left of the vertical dashed line can be located inside a small laboratory building or trailer. The antenna and the 915 MHz (UHF) transmit/receive unit shown to the right of the dashed line in Fig. 1 are located in the field. The UHF

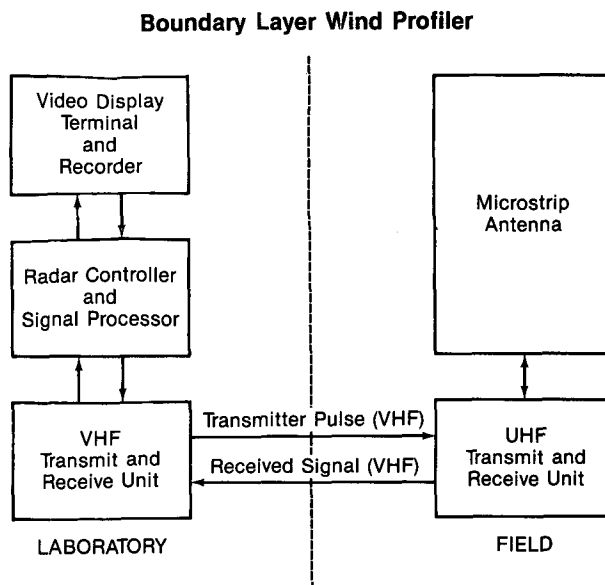


FIG. 1. Block diagram of the boundary layer wind profiler.

transmit/receive unit is mounted directly below the microstrip antenna.

In our design the entire 915 MHz system is located in the field. Both transmitted and received signals are converted to an intermediate frequency (IF) of 50 MHz (VHF in Fig. 1) to achieve lower transmission cable losses between the field and the laboratory/trailer. The 50 MHz IF was chosen to correspond to our conventional profiler frequency at our Pacific Island sites. In more general applications, any IF in the range of 30 to 70 MHz could be used.

#### b. The microstrip antenna

Boundary layer radar portability requirements dictate that the antenna should be rugged, lightweight, and easily transportable. The antenna should also be relatively inexpensive and be mounted low to the ground to suppress unwanted ground clutter returns. These requirements are best satisfied by the relatively new microstrip array technology. Accordingly, a prototype 91 cm × 91 cm center-fed printed-circuit array (based on a simple design shown by Ashkenazy et al. 1983) was developed. For our purposes, the printed-circuit board is mounted above a lightweight, rigid metal honeycomb panel that serves as a support structure for both the antenna and the antenna ground plane. The circuit board has been inverted (copper side toward the ground plane) so that the fiberglass substrate can serve as a tough, weatherproof cover.

The finished prototype antenna module, composed of 16 individual antenna "patches," has overall dimensions of 91 cm × 91 cm × 2 cm. The circuit board for each module (shown in Fig. 2) contains all requisite etched transmission lines and is phased for broadside

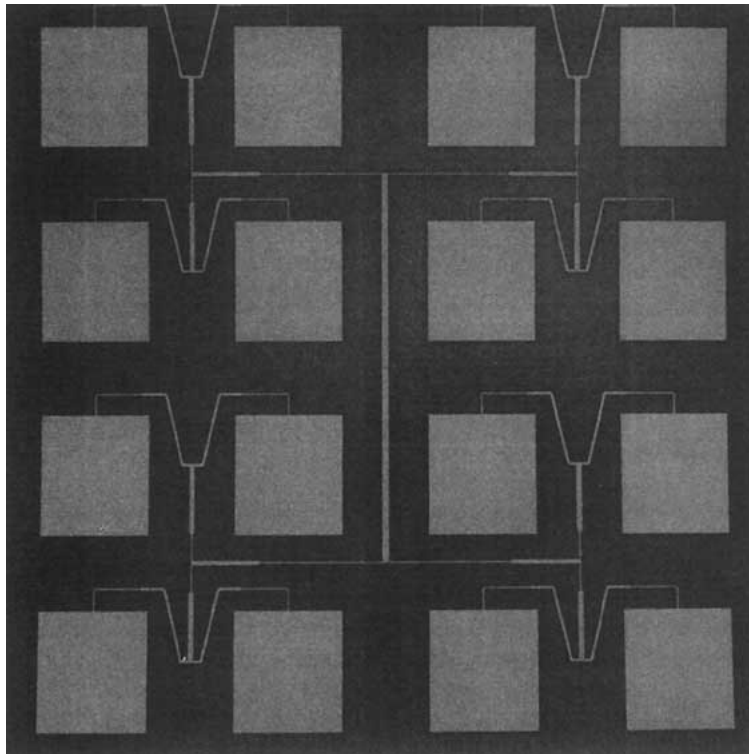


FIG. 2. Photograph of 91 cm  $\times$  91 cm circuit board showing 16 "patches" and microstrip transmission lines.

radiation. The RF connection to the module is accomplished by means of a single connector located on the back of the panel near the center. A single module has a measured half-power, one-way beamwidth of about  $18^\circ$ , as expected for a uniformly illuminated 91 cm aperture. Module efficiency is estimated to be about 80% based on measurements that compared the gain of the module with a reference dipole. Single modules can be connected together in a "building block" arrangement to achieve a narrower antenna beam and a commensurately larger area for particular wind profiling applications. Alternatively, we have fabricated single antenna panels as large as 91 by 273 cm, which consist of three 91 cm by 91 cm circuit boards mounted on a single large honeycomb panel.

To date we have operated the microstrip antenna panels in two test modes: 1) fixed in azimuth and elevation and 2) fixed in elevation ( $15^\circ$  off of the zenith) but rotated in azimuth using an inexpensive rotator designed for amateur radio use. Typical operation requires at least three beam positions in order to construct a vertical profile of both the horizontal and the vertical wind. (As will be discussed later, for 915 MHz operation during precipitation conditions, the measured vertical velocities are those of hydrometeors and are not clear air motions.)

In future designs the microstrip antenna technology could be combined with electronic beam-steering tech-

niques using phase shifters or other devices. We estimate that at this point the cost and complexity of a phase shifting network would more than double the cost of the antenna; this may be worthwhile for some applications, but for our preliminary studies we plan to use either multiple fixed-beam antennas with switching or a single panel that can be steered mechanically.

#### c. UHF transmit/receive unit

The 915 MHz transmit/receive unit shown on the right side of the block diagram in Fig. 1 is housed in a metal box mounted directly below the panel antenna. In this unit the low-level VHF drive signal is translated to 915 MHz using an 865 MHz local oscillator and then amplified to a peak power of about 100 W. The pulse length of the prototype transmitter can be varied from 0.5 to 2  $\mu$ s (radar range resolution of 75 to 300 m). The normal pulse repetition frequency (PRF) is 10 000 Hz (an unambiguous height coverage to 15 km). This combination of variable pulse widths and the fixed PRF results in a duty cycle of 0.5% to 2%.

#### d. VHF transmit/receive unit

The VHF (50 MHz) transmit/receive unit used in the prototype BLR system incorporates modules nor-

mally used in our conventional (50 MHz) profiler systems. Briefly, this unit provides a 50 MHz RF pulse (at the pulse rate and pulse width set by the radar controller) which is mixed up to 915 MHz by the UHF transmit/receive unit. In the receive mode, the VHF unit mixes the incoming 50 MHz returned signal (from the UHF transmit/receive unit) with a 50 MHz reference to produce the baseband quadrature outputs needed for Doppler analysis.

*e. Radar controller and signal processor*

The radar controller and signal processor employed for the prototype BLR system were adapted directly from our conventional VHF profiler system. Both controller and processor are on a single board mounted in the system computer (Carter et al. 1985). This signal processor has a minimum sample spacing of 1  $\mu$ s, which limits the resolution along the antenna beam to 150 m. Since the antenna beams are normally directed close to the zenith, this limit translates to a minimum height resolution of about 150 m.

Under normal operating conditions, as many as 30 heights can be sampled after each transmitted pulse. Consecutive samples at each height can be coherently integrated for a selected number of pulses. This process determines the effective data rate into the FFT (fast Fourier transform) processor and thereby determines the full-scale value of radial velocity at each height interval.

*f. Video display*

An example of the video display output of the BLR data obtained during clear air conditions at the Aeronomy Laboratory in Boulder, Colorado, on 28 August 1986 is shown in Fig. 3. This type of output displays contours of power spectral density (obtained from the spectral analysis) in terms of radial velocity and height. Height resolution is 145 m. The full-scale radial velocity is between +4.2 m s<sup>-1</sup> (toward radar) and -4.2 m s<sup>-1</sup> (away from radar). The polarity convention in Fig. 3 is opposite normal weather radar usage. This particular display represents a 2-min data sample. Power spectral density contour intervals are in 5 dB steps, with the weakest (outside) contour beginning 1 dB above the spectral density noise level. The S/N values listed on the left side of the figure are calculated from integrated signal and noise powers. In this example the interpulse period (IPP) is 100  $\mu$ s, the pulse width (PW) is 1  $\mu$ s, and the contour levels (first, increment) are 1 and 5 dB as explained above. The number of samples (NSAM 1) is 20, sample spacing (SPACE 1) is 1  $\mu$ s, and delay to the first sample (DELAY 1) is 1  $\mu$ s. The number of coherent integrations (NCI) or time domain averages is 188. The number of spectra averaged (NSP) or incoherent averages is 120, and the number of spectral points (NPTS) is 64.

The heavy dashed profile marks the first moment of the averaged spectra as a function of height. As we will show later, under clear air conditions, the first moment is a measure of the mean radial wind velocity. The 20

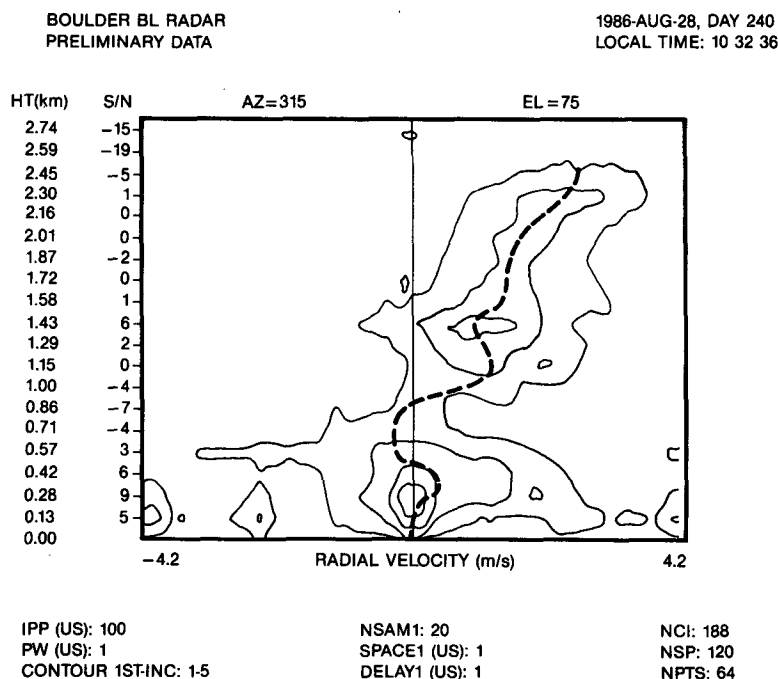


FIG. 3. Boundary layer radar video display on 28 August 1986.

averaged spectra (20 heights) that make up the video display contour plot (Fig. 3) are also recorded on magnetic tape in normal operation.

*g. Complete prototype BLR radar unit*

Figure 4 is a picture of a prototype antenna mounted near the Aeronomy Laboratory in Boulder, Colorado

(1600 m MSL). The UHF transmit/receive module is mounted under the antenna and is not visible. In this case the antenna consists of two  $91\text{ cm} \times 91\text{ cm}$  panels that have been inclined  $15^\circ$  from vertical. The array has been mounted on an inexpensive azimuth rotator. The antenna system is mounted inside a rudimentary "clutter fence" to reduce ground clutter from the

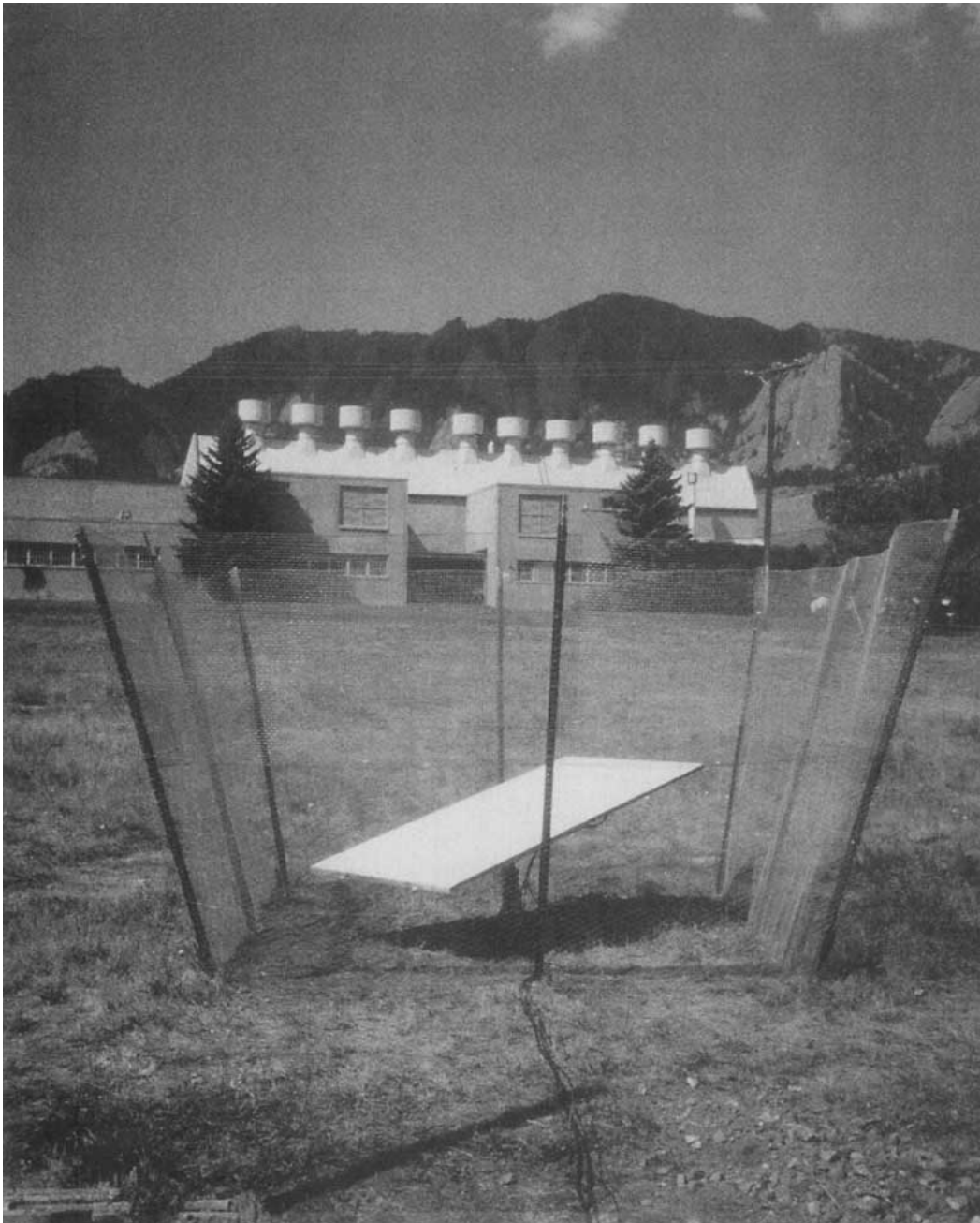


FIG. 4. Photograph of the prototype boundary layer radar mounted inside a rudimentary clutter fence. The antenna is fixed in elevation and rotates in azimuth. The UHF transmit/receive module is mounted on the back of the antenna panel.

buildings, power lines and mountains that are obvious in Fig. 4. Tests showed that the fence reduced the unwanted clutter by about 10 to 15 dB. In addition to ground clutter from fixed objects mentioned above, we also observed echoes from vehicular traffic passing within 50 m of the antenna. This intermittent source of clutter, when present, made it difficult to obtain usable wind measurements at the lowest heights. Birds passing through the beam provided an additional source of intermittent interference.

**4. Results**

The prototype BLR shown in Fig. 4 was operated intermittently from 11 August to 1 November 1986. During this period the normal operating procedure was to take spectral averages for 30- to 120-s periods at each of four azimuths separated by 90°. A schematic of the beam positions is shown in Fig. 5. Positions 1 and 2 correspond to "opposed" azimuths as do positions 3 and 4. In some instances, the opposed azimuths were situated in the zonal (E-W) and meridional (N-S) directions but at other times they were situated in the NE-SW and NW-SE directions as indicated in Fig. 5.

Boundary Layer Radar  
Antenna Beam Positions

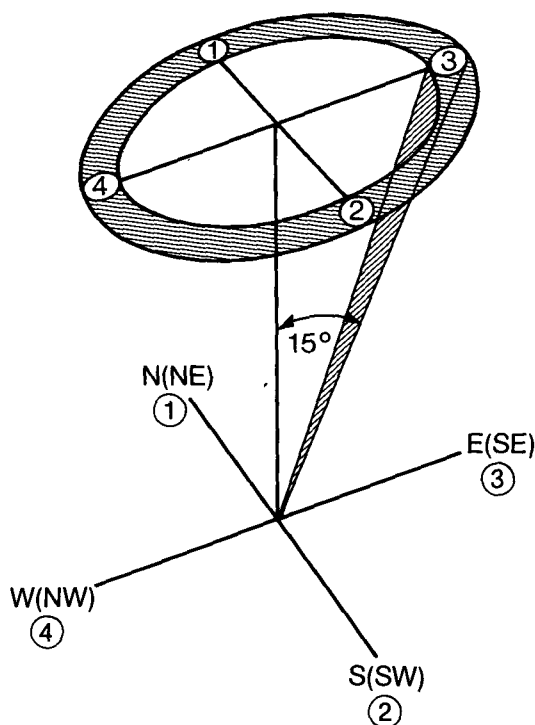


FIG. 5. Schematic of the boundary layer radar antenna beam positions.

Provided that the wind field can be assumed to be uniform (no divergence) over the dimensions shown by the annulus in Fig. 5, it is possible to obtain horizontal wind vectors in the two planes containing the opposed sets of radial drifts. It is also possible to obtain two independent measurements of the vertical velocity in this operating mode if we assume no divergence. For example, let beams 3 and 4 be inclined 15° east and west of vertical as shown by the nonparenthetical case in Fig. 4. Similarly, let beams 1 and 2 be inclined 15° north and south of vertical. Under these conditions, the zonal (*u*), meridional (*v*), and vertical wind (*w*) can be obtained from

$$\begin{aligned}
 u &= (V_{r4} - V_{r3})/2 \sin(15^\circ) \\
 v &= (V_{r1} - V_{r2})/2 \sin(15^\circ) \\
 w &= -(V_{r4} + V_{r3})/2 \cos(15^\circ) \\
 &= -(V_{r1} + V_{r2})/2 \cos(15^\circ)
 \end{aligned}$$

where *V<sub>m</sub>* refers to the measured radial drift velocity in the *n*th beam (*n* = 1, 2, 3, 4) shown in Fig. 5. Note that the two measurements of *w* are independent. In this simplified treatment we have assumed that the wind field is uniform (no divergence) over the antenna beams. We note, however, that the beam configuration used here (Fig. 5) does not allow vertical velocity and divergence to be strictly separated (Browning and Wexler 1968). When the opposed azimuth measurements are not made in the zonal or meridional planes (see, for example, the directions within parentheses in Fig. 5), the zonal and meridional winds can be obtained via a simple trigonometric transformation.

Sample wind profiles at the Colorado site were obtained under a variety of conditions, ranging from absolutely clear conditions to heavy thundershowers. These conditions included a case where snow changed to rain 1 km above the radar. Another situation involved the observation of a strong lee-wave rotor above the radar (not discussed here).

In general the BLR was able to observe up to about 1500 m in clear air with 150 m height resolution and an average power aperture product of 2 W m<sup>2</sup>. On some occasions the height coverage was higher or lower, in agreement with other radar studies (Nastrom et al. 1986; Frisch et al. 1986) which have shown that the extreme range of radar reflectivity covers more than two orders of magnitude. As expected, the maximum observable height range increased dramatically under precipitation conditions.

*a. Wind profiles during clear sky conditions*

Figure 6 shows an example of data obtained during clear sky conditions when the reflectivity was higher than usual. On this day the wind could be measured up to an altitude of 2650 m above ground with 150 m

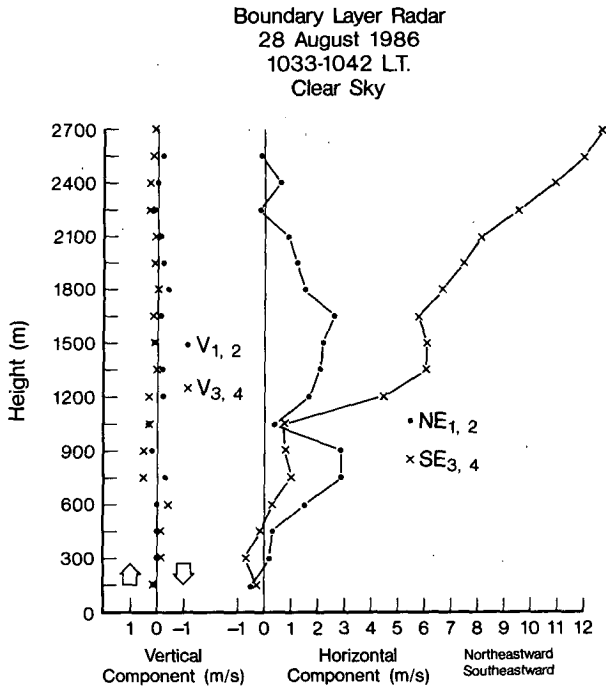


FIG. 6. Profiles of vertical and horizontal winds obtained on a clear day.

resolution. The wind profile was obtained from measurements obtained along four beams (as described previously) over the period 1033–1042 LST. In this instance the opposed azimuths were aligned in the NE–SW and SE–NW directions (cf, Fig. 5).

The NE–SW and SE–NW horizontal wind components are shown on the right side of Fig. 6. The horizontal wind was very light near the surface and increased with altitude. The wind at the highest observed altitude was blowing toward the southeast at  $12 \text{ m s}^{-1}$ .

Two measurements of the vertical wind component are shown on the left side of Fig. 6, with the vertical winds determined from beam positions 1 and 2 ( $V_{1,2}$ ) indicated by dots, and the winds from beam positions 3 and 4 ( $V_{3,4}$ ) indicated by  $\times$ . The vertical wind profiles obtained from the two pairs of opposing beams generally agree to within about  $\frac{1}{4} \text{ m s}^{-1}$  except at the 750 and 1200 m levels. The inferred vertical component under these conditions is close to zero.

On this day, the  $S/N$  ratios on azimuths nearly along the wind direction (SE and NW) were observed to be some 5 to 10 dB higher than on azimuths directed across the wind direction (NE and SW). This difference persisted for several hours. Although it is tempting to postulate a vector relationship between wind shear and echo strength, no definite explanation for this difference is immediately obvious. Similar differences were noted on one other clear-sky day, but, in general, the clear sky reflectivity is observed to be independent of azimuth.

*b. Wind profiles during snow/rain conditions*

As already noted, the 915 MHz radar is much more sensitive to hydrometeor scatter than the 50 MHz radar. Figure 7 shows an example of vertical and horizontal velocity components obtained in October 1986 with 150 m height resolution when light rain was falling at the BLR. In this measurement the opposed azimuths were aligned E–W and N–S (Fig. 5). At the time of this observation, snow was observed to be accumulating on the top of nearby Green Mountain, the highest peak appearing in Fig. 4 (which is about 1000 m higher than the BLR). The height coverage for both the horizontal and vertical data extends considerably higher than in the clear air case (Fig. 6) due to the larger reflectivity of snow and rain.

Since the dominant scatterers in this instance are hydrometeors, the horizontal components shown on the right side of Fig. 7 are due to the horizontal advection of the hydrometeors by the horizontal winds. Although we have no independent measurement of the horizontal wind components during this period, the direction and magnitude of the deduced wind profiles appear reasonable. The rain on this day was associated

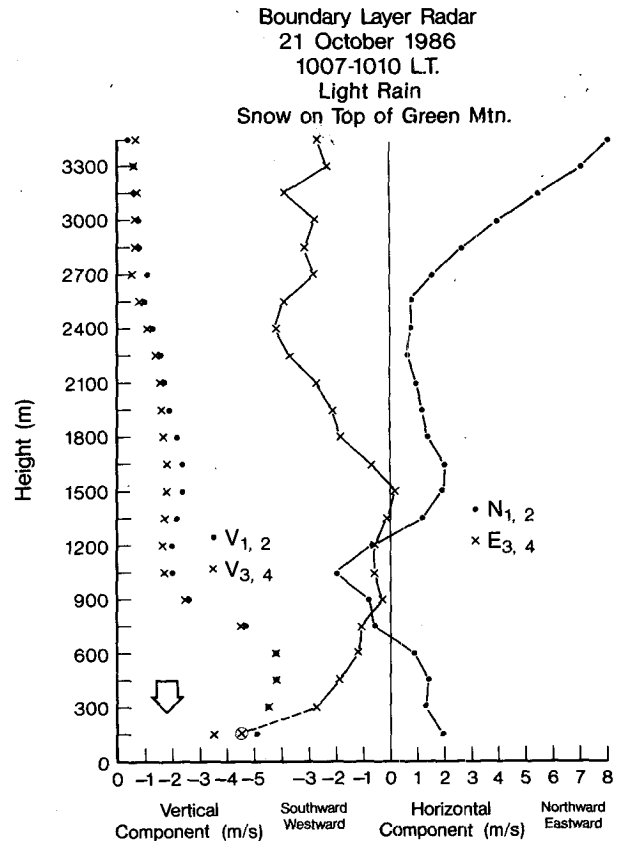


FIG. 7. Profiles of horizontal winds and hydrometeor fall speeds (vertical component) on a day with light rain at the ground. Note the increase in fall speed below 1000 m.

with an upslope condition, and the  $E_{3,4}$  component (×) shows a westward wind of over  $5 \text{ m s}^{-1}$  at a height of 150 m (circled ×) decreasing to near zero at 900 m.

The vertical motions shown on the left of Fig. 7 in this case are due to the fall speed of the scattering hydrometeors. Again  $V_{1,2}$  and  $V_{3,4}$  agree well, except at a height of 150 m and at intermediate heights from about 1200 to 1800 m. In this case, the vertical components change markedly with height. Above about 1000 m the fall speed is about  $2 \text{ m/s}$ , decreasing to less than  $1 \text{ m s}^{-1}$  at higher heights. An abrupt change in fall speed occurred at 1000 m, with the fall speed increasing with decreasing height to  $6 \text{ m/s}$  at 600 m and below. The transition region is apparently due to the hydrometeors changing from snow/ice to rain at about 1000 m above the radar. This interpretation would be consistent with the conditions observed visually and is further supported by the observation of a relative peak in reflectivity that occurred at 900 m. This feature is similar to the "bright band" observed at shorter wavelengths that has been shown to coincide with the melting layer. Lhermitte and Atlas (1963) showed that the particle fall speed increased below this layer in much the same way as shown in Fig. 7.

*c. Wind profiles during a thundershower*

A set of wind profiles observed during a thundershower on the afternoon of 19 August 1986 (height resolution 150 m) appears in Fig. 8. Heights above 4350 m are not shown in this figure, although the echoing region in fact extended to higher heights. Indeed, during several similar afternoon thundershowers, we have observed echoes up to about 8000 m above the surface. The winds at a height of 300 m are directed toward the east-northeast at about  $13 \text{ m s}^{-1}$ .

The hydrometeor fall speeds shown on the left side of Fig. 7 maximize at about  $10 \text{ m s}^{-1}$  at a height of about 2000 m. In this case, the two independent estimates of vertical motion,  $V_{1,2}$  and  $V_{3,4}$ , agree less well than they did under either clear sky or light rain conditions (Figs. 6 and 7). We tentatively attribute this difference to space/time variations in the thundershower.

*d. Preliminary tropical tests*

In November 1986 a preliminary test of the BLR was carried out near the equator south of Hawaii at Christmas Island, Republic of Kiribati. For this test a single  $91 \text{ cm} \times 91 \text{ cm}$  antenna panel was placed on the ground and tipped  $15^\circ$  from the zenith toward the east. The BLR was operated in this configuration for about  $1\frac{1}{2}$  days. Using a peak transmitted power of 100 W (1 W average), a  $1.0 \mu\text{s}$  pulse (150 m resolution) and a 60 second observing period, the BLR observed essentially continuous echoes to a height of 1800 m. On several occasions echoes were observed up to 2400 m for approximately 1 h periods.

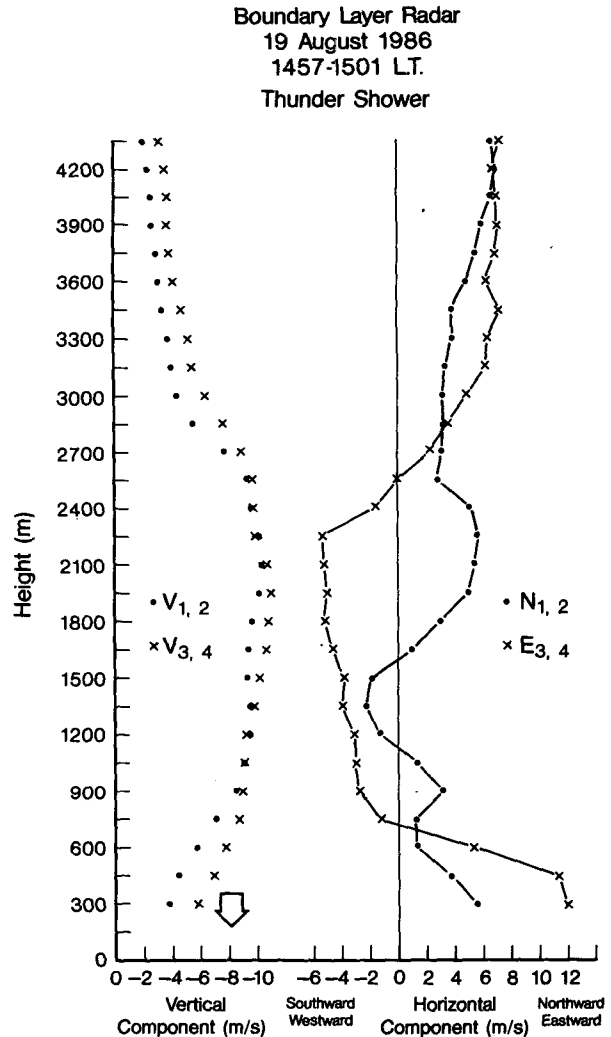


FIG. 8. As in Fig. 7 except taken during a thundershower.

Since the 50 MHz radar at Christmas Island typically observes useful echoes down to a minimum altitude of 1700 m, it was possible to overlap the 50 MHz and 915 MHz profiles. A "hybrid" wind profile obtained in this way on 8 November 1986 is shown in Fig. 9. The profiles obtained by the two radars are separated in time by several hours because of the time necessary to change from one radar system to the other in this preliminary experiment. The BLR values have been arbitrarily reduced by 20% in order to achieve the best "match" in the intersection region of the two profiles. The difference between the two profiles in the intersection region either arises from a temporal variability of the zonal wind field during the several hour change-over period, or to errors in the BLR profile arising from the relatively broad beamwidth of the single panel antenna. In the event that the problem did arise from the broad beamwidth antenna, such errors will be minimized in future systems by the use of larger antennas





several thousand meters on a continuous basis with good time and altitude resolution.

*Acknowledgments.* We greatly appreciate the assistance of Philipp Currier who helped in constructing and testing the BLR. We also thank R. Strauch for useful discussions and the loan of some 915 MHz equipment. This work was partially funded by NOAA's TOGA (Tropical Oceans and Global Atmospheres) program.

#### REFERENCES

- Ashkenazy, J., P. Perlmutter and D. Treves, 1983: A modular approach for the design of microstrip array antennas. *IEEE Trans. Anten. Prop.*, **AP-31**, 190-193.
- Balsley, B. B., and K. S. Gage, 1982: On the use of radars for operational wind profiling. *Bull. Amer. Meteor. Soc.*, **63**, 1009-1018.
- Browning, K. A., and R. Wexler, 1968: The determination of kinematic properties of a wind field using Doppler radar. *J. Appl. Meteor.*, **7**, 105-113.
- Carter, D. A., A. E. Ayers and R. P. Schneider, 1985: A single-board preprocessor and pulse generator. *Third Workshop on Technical and Scientific Aspects of MST Radar*, Aguadilla, Puerto Rico.
- Frisch, A. S., B. L. Weber, R. G. Strauch, D. A. Merritt and K. P. Moran, 1986: The altitude coverage of the Colorado wind profilers at 50, 405 and 915 MHz. *J. Atmos. Oceanic Technol.*, **3**, 680-692.
- Fukao, S., K. Wakasugi, T. Sato, S. Morimoto, T. Tsuda, I. Hirota, I. Kimura and S. Kato, 1985: Direct measurement of air and precipitation particle motion by very high frequency Doppler radar. *Nature*, **316**, 712-714.
- Gage, K. S., W. L. Ecklund, A. C. Riddle and B. B. Balsley, 1986: Objective tropopause height determination using low-resolution VHF radar observations. *J. Atmos. Oceanic Technol.*, **3**, 248-251.
- Lhermitte, R. M., and D. Atlas, 1963: Doppler fall speed and particle growth in stratiform precipitation. *Proc. Tenth Weather Radar Conf.*, Boston, Amer. Meteor. Soc., 297-302.
- Nastrom, G. D., K. S. Gage and W. L. Ecklund, 1986: Variability of turbulence, 4-20 km, in Colorado and Alaska from MST radar observations. *J. Geophys. Res.*, **91**, 6722-6734.
- Strauch, R. G., D. A. Merritt, K. P. Moran, K. B. Earnshaw and D. Van de Kamp, 1984: The Colorado wind-profiling network. *J. Atmos. Oceanic Technol.*, **1**, 37-49.
- , —, and —, 1985: Radar wind profilers in the Colorado network. NOAA Tech Memo. ERL WPL-10, NOAA/ERL Wave Propagation Laboratory, 73 pp.
- Wuertz, D. B., B. L. Weber, R. G. Strauch, A. S. Frisch, C. G. Little, D. A. Merritt, K. P. Moran and D. C. Welsh, 1988: Effects of precipitation on UHF wind profiler measurements. *J. Atmos. Oceanic Technol.*, **5**, in press.